Supplementary Materials

1. Investigation of movement-induced convection flow

In our experiments, we primarily investigated the following three aspects:

1) mixing effects in liquefied (0.9% saline) vs. regular vitreous humor (glycerol 20.2 wt% mixture)
2) mixing effects after 10 cycles vs. 200 cycles of lateral movements
3) varied injection sites

Our experimental results show that rapid eye movements can induce four circulations in the liquefied vitreous humor, as shown in the PIV plot (Fig. S1a). Similarly, we also conducted a particle pathline tracking, starting when the lateral movement ended (Fig. S1b). We can conclude from Fig. S1 that: 1) particles can easily become trapped in one of the circulations, preventing them from reaching the target site, and 2) movement-induced convection flow does not sustain for long after the movement ends. For example, once the movement stopped, the circulations continued for about 15 s and then decayed completely.

In regular vitreous humor, this circulation phenomenon was barely observed. We performed particle pathline tracking for particle trajectory after 10 cycles (Fig. S2a) and 200 cycles (Fig. S2b) of lateral movements, respectively. The particles exhibited very little motion in both cases.

The above-mentioned phenomenon can be explained by calculating the Reynolds number (Re = $\frac{UD}{\nu}$,where $\nu = \frac{\mu}{\rho}$). Based on our analysis, the critical Reynolds number for activating the circulation is somewhere between 200 and 400. Since D is determined by individual patient eye morphology, and ν is a flow property that varies among different individuals and ages, only U can be controlled. However, it is impossible to ask the patients to continuously move their eyes at a high speed, especially after a painful intravitreal injection session. Furthermore, the mixing effects from the four circulations are not effective enough to deliver the drug from the injection site to the back of the eye. Therefore, using the thermal effects introduced in our work is simpler and more practical in promoting better drug mixing and delivery in the eye.

(a) (b)

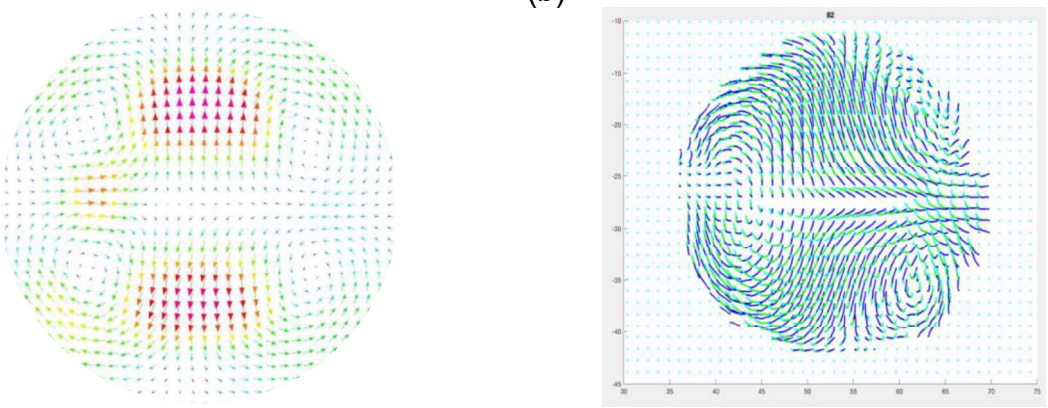

Figure S1. Movement-induced mixing effects in liquefied vitreous humor (0.9% saline). (a) PIV velocity fields. (b) Particle pathline tracking, begun after lateral movements stopped. The dark blue line indicates particle movements during the first 5 s, the green line indicates particle movements during the second 5 s, and the light blue line indicates particle movements during the last 5 s.

(a) (b)

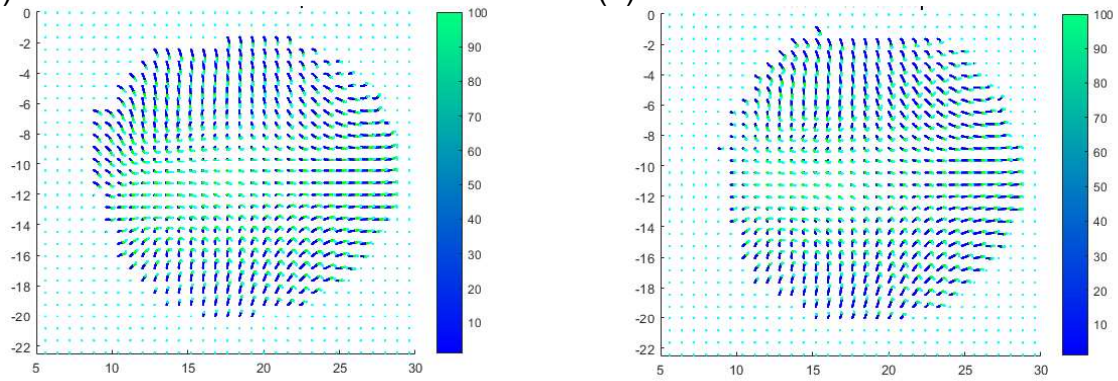

Figure S2. Particle pathline tracking (begun after 10 (a) or 200 (b) lateral movements were completed). The dark blue line indicates particle movements during the first 5 s, the green line indicates particle movements during the second 5 s, and the light blue line indicates particle movements during the last 5 s. (a) After 10 cycles of lateral movements; (b) After 200 cycles of lateral movements.

2. **Monitoring temperature using a thermal camera and a thermometer**

We used an FLIR SC6700 infrared camera (equipped with FLIR Exam IR software) to monitor the real-time temperature variation throughout 1 h of heating (Fig. S3a). We observed that the overall temperature increase was around 2 °C. This indicates that although air is a good insulator, it is conductive enough for our purposes.

To further confirm this observation, we used an Omega Engineering HH806AU thermometer and surface thermocouple with self-adhesive backing (Type k) to monitor temperature variations. Temperature readings were taken at two locations: a reference point on the heating element and the location of the “macula” (Fig. S3b). Since the heating element was made of two metals, steel and aluminum, in different geometries, as indicated in the main text, there was a consistent temperature difference along the heating element. This temperature difference was pre-calibrated and the temperature reading at the reference point was correlated with the temperature reading at the contact surface between the eye model and the heating element. For example, a temperature reading of 42 °C at the reference point corresponds to 32 °C at the contact surface. Temperatures at the reference point and the “macula” location were measured using two surface thermocouples throughout a total of 1 h of heating (Fig. S3c). Overall, observations of temperature increase at the “macula” location is consistent with our previous observations from using the infrared camera.

To compare the domain insulation in our setup with that of a real eye, we have summarized the coefficients of thermal conductivity in Table S1. Vitreous humor is the primary fluid that fills the space between the lens and the retina. Its coefficient of thermal conductivity is very close to that of the model mixture in our study. The lens, sclera, and cornea are the surrounding tissues and can affect heat transfer to the vitreous humor, just like the glass container in our study. Glass has a higher thermal conductivity compared to these tissues.

(a)

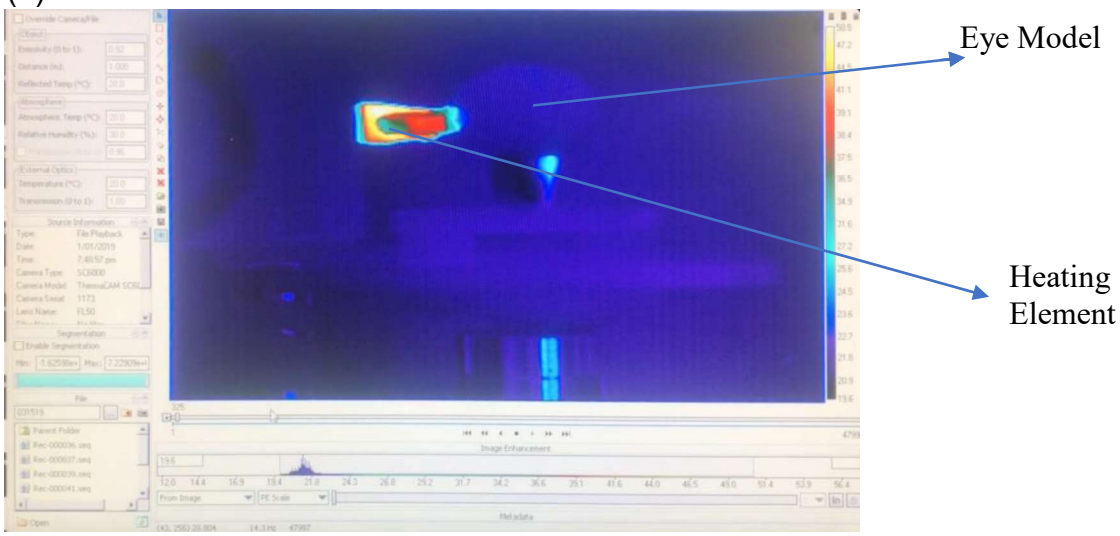

(b)

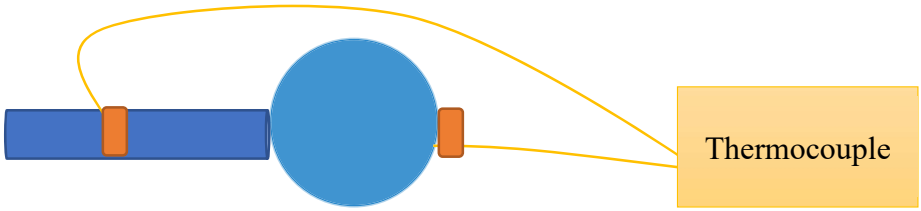

(c)

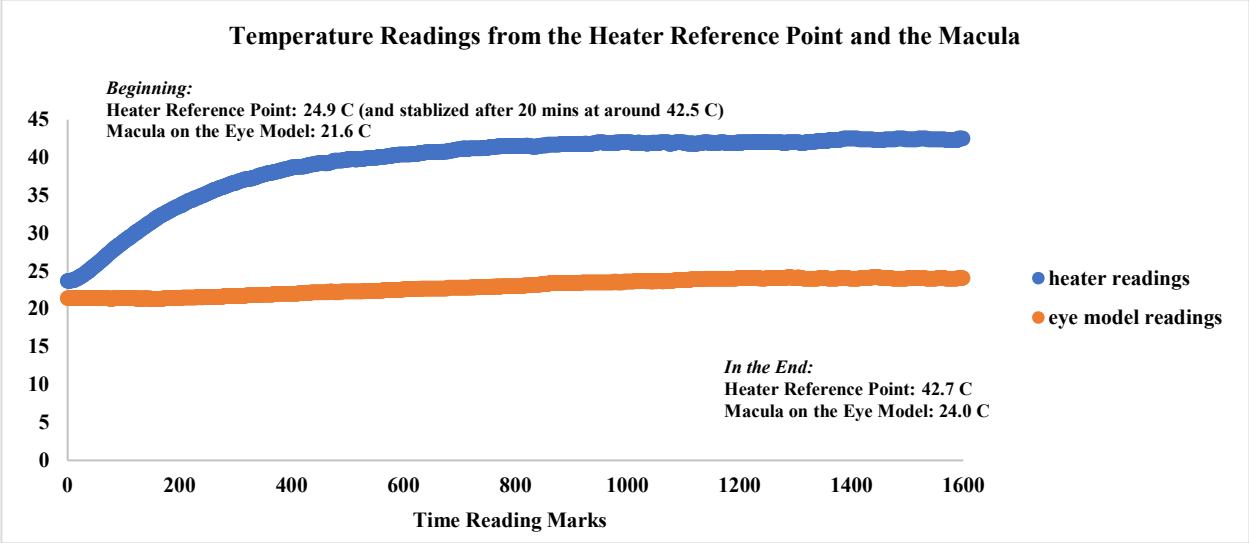

Figure S3. Temperature monitor results summary. (a) Real-time monitoring using an FLIR SC6700 infrared camera. (b) Schematic of the locations (marked in orange) of the reference point and the macula. (c) Temperature recordings from the thermometer and thermocouple at the two locations: the reference point on the heating element and the "macula" location on the eye model. Temperature reading interval: 3 s. Total duration: 1600 × 3 s = 4800 s.

Table S1. Summary of coefficients of thermal conductivity

	Coefficient of Thermal Conductivity ($W\ m^{-1}K^{-1}$)
Air at 20 °C	0.026
Glass, ordinary	0.800
20.2 wt% Glycerol at 20 °C	0.556
Vitreous humor	0.594
Cornea	0.580
Lens	0.400
Sclera	0.580

Data source:

- Engineering ToolBox, (2009). Air - Thermal Conductivity. [online] Available at: https://www.engineeringtoolbox.com/air-properties-viscosity-conductivity-heat-capacity-d_1509.html [Accessed 20 Feb. 2020].
- Narasimhan A, Jha KK. Bio-heat transfer simulation of square and circular array of retinal laser irradiation. Front Heat Mass Transfer. 2010;53:482–90. [Google Scholar]

- Cvetkovic M, Poljak D, Pretta A. Thermal Modeling of the Human Eye Exposed to Laser Radiation. IEEE SoftCOM 2008. 16th Int. Con., Sept. 2008.
- Young, Hugh D., University Physics, 7th Ed., Addison Wesley, 1992.

3. **Refractive index issue discussion.**

We are aware of the importance of matching the refractive index of the working fluid with that of the glass. In our experiment, the refractive index is 1.36 for the working fluid (20.2 wt% glycerol) and 1.46 for fused quartz glass. The refractive index can be matched by immersing the glass globe in a viewing box that is filled with the working fluid to fix the refractive index issue. However, for our design, this is difficult to achieve. Because when a glass globe is immersed in the fluid, it would be challenging to ensure the controlled local heating like the one we did in this setup.

To understand the impact of not immersing the globe in a fluid-filled viewing box, we repeat the experiment with the face-up heating position both with and without a fluid-filled viewing box. For a face-up heating position, the heater is placed on the top of the glass globe, so a small area at the very top of the eye model is exposed to air to facilitate the application of a local heating, while the rest of the eye model is immersed in the working fluid. In parallel, another experiment is performed without having the eye model immersed in the working fluid, which is the same as the one we did in our study. The results are summarized in Fig. S4. The percentage difference is in the range of 12-20% and the general vorticity increasing trend is consistent. This experimental result confirms that the potential error caused by an unmatched refractive index will not change our conclusion.

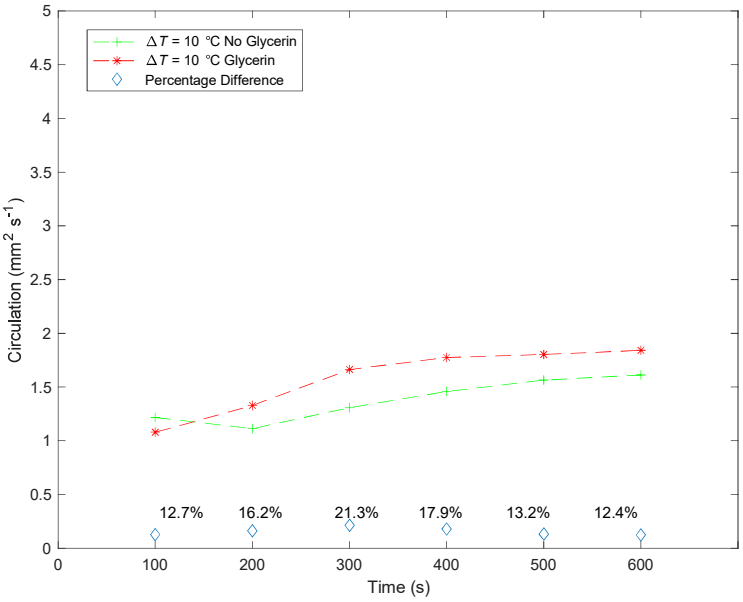

Figure S4. Absolute value of the circulation calculated from PIV data. The green cross line: results from not having the eye model in the working fluid; the red star line: results from having the eye model immersed in the working fluid. Diamond marks: percentage difference as calculated by $\frac{\text{Vorticity}_{\text{glycerin}} - \text{Vorticity}_{\text{no glycerin}}}{\text{Vorticity}_{\text{glycerin}}}$

4. **A comparison between fluorescein powder and anti-VEGF drug.**

The clinical product of anti-VEGF drug is a sterile, colorless to pale yellow aqueous solution in a single-use prefilled syringe/glass vial. Water is the primary carrier of this drug in the delivery process. [Note: Taking LUCENTIS® (ranibizumab injection, a type of anti-VEGF) as an example, each product is designed to deliver 0.05 mL of 10 mg/mL or 6 mg/ml aqueous solution with 10 mM histidine HCL, 10% α,α-trehalose dehydrate, and 0.01% polysorbate 20.]

In our study, fluorescein powder (1.602 g/ml) is mixed with water at 0.2 g/ml. The fluorescein aqueous solvent is then mixed with either 11.2 wt% glycerol or 33.6 wt% glycerol at a 1:50 volume ratio (1.9 vol% fluorescein aqueous solvent). Glycerol/water mixture is the main carrier of the “drug” in this study.

Therefore, we have compared the important properties of water and the glycerol/water mixtures in Table S2 (selected data from updated Table 1 in the manuscript). We didn’t choose to use water as the main carrier for two reasons: 1) to minimize the variables introduced in the study, adding glycerol/water mixture to glycerol/water mixture is an ideal option; 2) mixing glycerol and water at different ratios allow us to make controllable changes to density/viscosity.

Table S2. Material properties of vitreous and materials used in the current study

Material	Viscosity at 20°C (mPa s)	Density (kg m^{-3})	Thermal expansion coefficient (at 20 °C)	Refractive index	Coefficient of thermal conductivity (20 °C) (W m^{-1} K^{-1})
Water	1	997.0	2.1×10^{-4}	1.33	0.594
33.6 wt% glycerol	2.7	1081.5	3.9×10^{-4}	1.37	0.515
11.2 wt% glycerol	1.3	1024.5	2.6×10^{-4}	1.35	0.591